

# Miniature Illuminator for Laser Doppler Velocimeter Assembled on Micromachined Silicon optical bench.

A. Ksendzov<sup>a</sup>, R.D. Martin<sup>b</sup>, D. Modares<sup>c</sup>, M. Gharib<sup>d</sup>

(a) Jet propulsion Laboratory, California Institute of Technology, Pasadena, CA 91109

(b) W.L. Gore & Associates, Newark, DE 19713

(c) Dept. of Aeronautics, California Institute of Technology, Pasadena, CA 91125

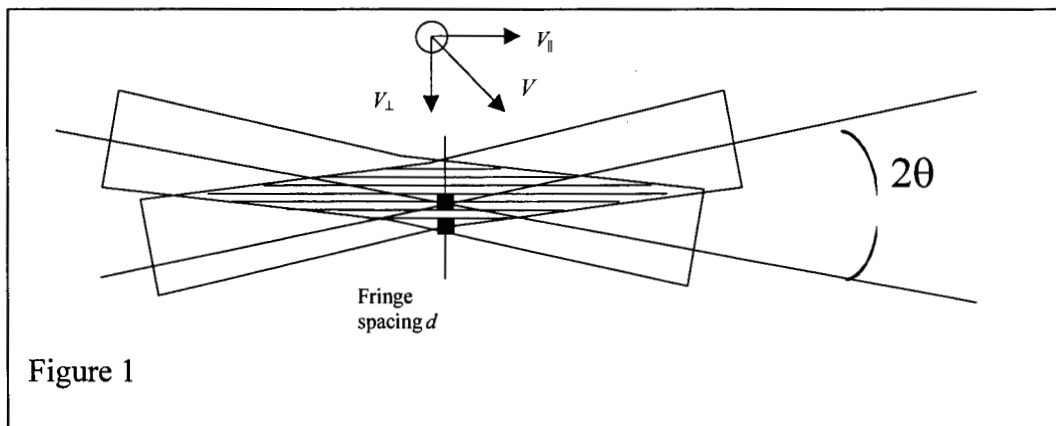
(d) Dept. of Aeronautics, California Institute of Technology, Pasadena, CA 91125

## Abstract

We have built a miniature illuminator for Laser Doppler velocimeter on micromachined optical bench utilizing a novel optical scheme. We used two intersecting coherent beams from the two opposing facets of semiconductor laser die to form a standing interference pattern needed for the particle detection and velocity measurement. Such devices are of interest to NASA for investigating wind patterns and dust loading on planets with atmosphere. They can be applied to other problems where the liquid or gas flux must be characterized without disturbing the flow. In addition, the small probe volume makes possible local flow characterization and profiling. The device fabrication, and the results of the fringe characterization and velocity measurements are presented and discussed.

## Introduction

The laser Doppler velocimeter can be used for remote contactless velocity measurement of objects moving through a transparent medium. The measurement utilizes two intersecting coherent light beams producing a standing fringe pattern, as illustrated in Figure 1.



An object crossing fringes gives rise to light scattering modulated in time with the frequency determined by both the object velocity and the fringe spacing. The fringe spacing  $d$  is given by the following expression:

$$(1) d = \lambda / (2 \sin \theta),$$

where  $\lambda$  is the wavelength of the light source, and  $2\theta$  is the angle between the crossing beams. Therefore the observed modulation frequency  $f$  is

$$(2) f = 2V_{\perp} \sin \theta / \lambda,$$

where  $V_{\perp}$  is the velocity component normal to the fringes.

The uses of such devices include contactless liquid and gas velocity measurements. In all applications the presence of light scatterers such as dust particles in air flow<sup>1</sup> or red blood cells travelling with blood stream<sup>2</sup> facilitates measurements. The possibility of achieving a small probe volume is a useful feature allowing for local velocity measurements needed to measure flow profiles as well as monitoring flow in small volumes. In addition, reducing the probe volume increases the intensity of the scattered light and facilitates detection of smaller particles.

Earlier approaches utilized light from one laser die facet and used a beamsplitter<sup>1</sup> or a grating<sup>3</sup> to create two intersecting coherent beams. In our view, the use of coherent beams from two opposite laser die facets simplifies the device fabrication and alignment. Such scheme has been validated recently by Ito *et al*<sup>4</sup> who fabricated a miniature integrated velocimeter as a planar structure less than 1 mm<sup>2</sup>. The applications of their device however seem to be limited to objects placed very closely to the velocimeter due to lack of light focusing.

This work was sponsored by NASA as technology validation for a miniature anemometer to be used in wind and dust particle studies on Mars and other planets. Thus the goal is an illumination bench that produces a small (tens of microns across) sensing volume a few centimeters away from the bench. Since for the planetary mission use small size is important, we pursued the use of a micromachined Si bench as a means of aligning all optical elements, including a flip-chip mounted semiconductor laser die.

The scope of this project was limited to building and testing the illumination bench. A complete miniature device should include the detector and detector optics located on the same bench. We chose to use red lasers for the ease of alignment. While low power of such lasers may be sufficient for some applications, more powerful near infrared laser dice should be used to detect small particles.

### **Bench layout, fabrication, and alignment**

The bench photograph is presented in Figure 2. The light emitted from the facets of the die is collected by two GRIN lenses (G1, G2), sent to two opposing mirrors (M1 and M2) and is focused at the intersection point approximately 23 mm above the bench.

To facilitate easy alignment, we used two independent Si substrates: the mirrors are mounted on the lower substrate, while the die and the GRIN lenses are mounted on the top bench. The mirrors were affixed with epoxy in shallow recesses etched in the bottom substrate for the part registration. The top bench has Au/Sn solder bumps [Ref. 5] for the laser die placement and etched V-grooves

[Ref.6] that provided for the GRIN lens axial positioning. While the V-groove depth and the bump height were matched to provide the correct vertical registration, the horizontal alignment was achieved by attaching the laser die with a precision flip-chip

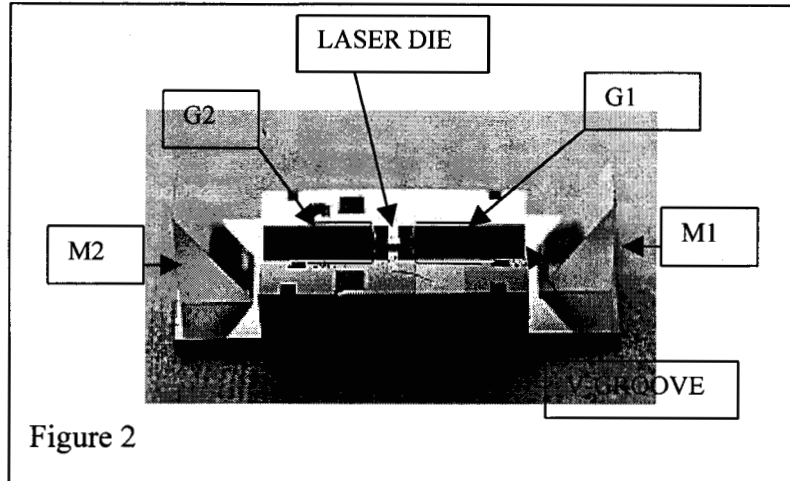


Figure 2

bonder (Research Devices MG-8). We used alignment marks defined lithographically simultaneously (on the same layer) with the V-groove outline. The bonder provides lateral placement accuracy of  $\pm 1.5 \mu\text{m}$ . We have used the AuSn bumps as described in Ref. 5. The recommended temperature for the die attachment is 315 C (see Ref 5). We have used the tool temperature of 370 C to which we arrived by experimentation since the bonder provides no direct measurement of the solder bump temperature.

The uncoated laser dice used in this project were provided by SDL, Inc. They lase at 660 nm at room temperature and emit single mode in a wide range of currents. This range for the die used in the reported device is approximately 40-75 mA (it is somewhat die-specific). The use of uncoated dice will probably lead to low reliability of this device. However, obtaining custom coated dice would be prohibitively expensive for this project.

The device was mounted on a rotation stage so that the top bench with the die and GRIN lenses could be rotated versus the bottom substrate with the mirrors to effect the beam crossing. The GRIN lenses were placed in V-grooves and moved axially using micropositioners. We monitored the beam intersection area during alignment by projecting it onto a CCD camera focal plane through a microscope objective. Once the best alignment was achieved, we 'tacked' the GRIN lenses to the upper bench and the upper bench to the lower substrate using UV-curable epoxy.

### Test results and discussion

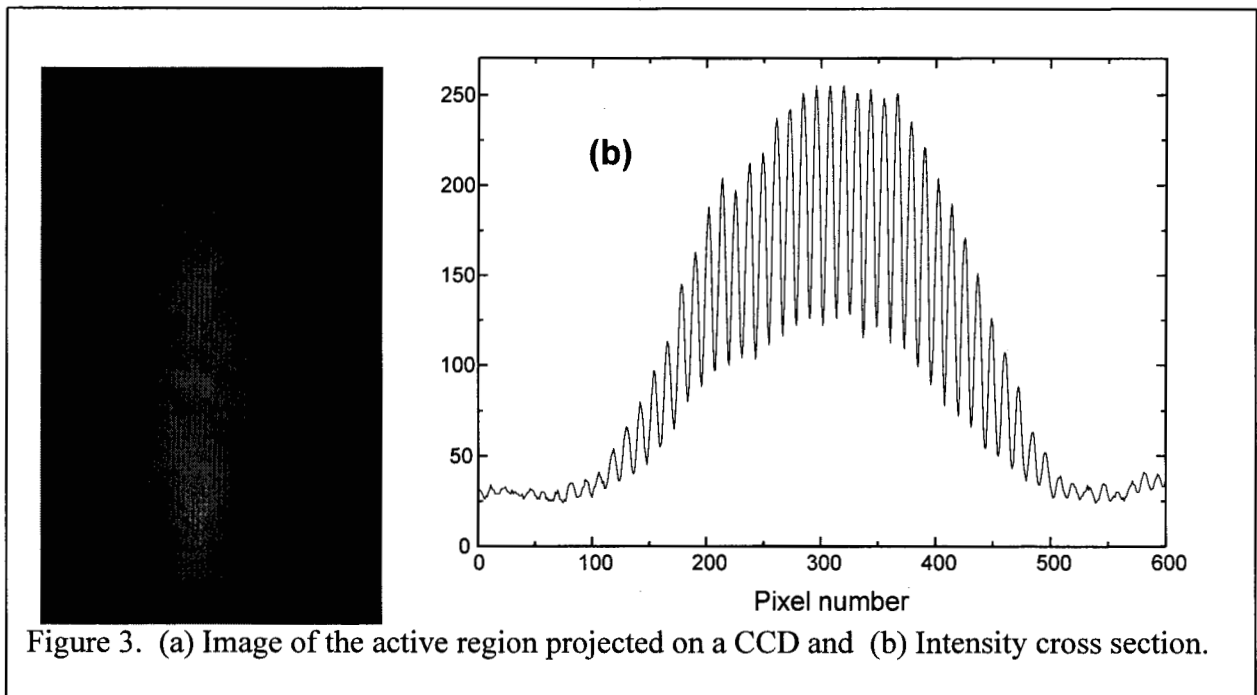
In order to validate the design and the alignment procedure we have performed two tests. Firstly, we have imaged the active region of the illuminator and analyzed the cross section. Secondly, we have performed the velocity measurement calibration. The calibration data is consistent with predictions based on calculations using design parameters.

### *Active region analysis*

To analyze the active region, we imaged it through a microscope objective with N.A. of 0.85, large enough to collect all the light. The image was projected onto the focal plane of a CCD camera and was grabbed using a National Instruments image board. The image is presented in Figure 3(a) and the intensity cross section is shown in Figure 3b.

The expected cross section of the beam waist is an oblong shape determined by the angle  $\theta$  and by the laser beam divergence in the vertical and horizontal planes. The evaluation of the expected active area size started with measuring the divergence of the laser beam ( $38^\circ \times 13^\circ$  full width @  $1/e$  power). Then the beam convergence after the GRIN lens was computed using angular magnification of  $1/17$ . Finally, the beam waist size along the wide and narrow dimensions was calculated using expressions for Gaussian beams<sup>7</sup>. Taking into account the angle between the beams ( $\theta=20^\circ$ ), the active area cross section was estimated at  $6 \times 18 \mu\text{m}$ .

The beam cross section in Figure 3b is approximately 25 fringes wide at  $1/e$  level. Since the calculated fringe spacing is  $0.95 \mu\text{m}$ , that translates into the narrow dimension



of  $24 \mu\text{m}$ , much larger than predicted. We believe this discrepancy is due to non-ideal focusing. Using Figure 3a, the wide dimension of the active area is approximately  $140 \mu\text{m}$ , much larger than expected from the 3:1 aspect ratio predicted above. We believe this is due to misalignment of the two laser beams. Such misalignment may as well explain the 1:1 ratio of the fringe depth to the fringe minima whereas full extinction at the minima were expected.

### *Velocity calibration*

The velocity measurements were calibrated using a motorized translation stage

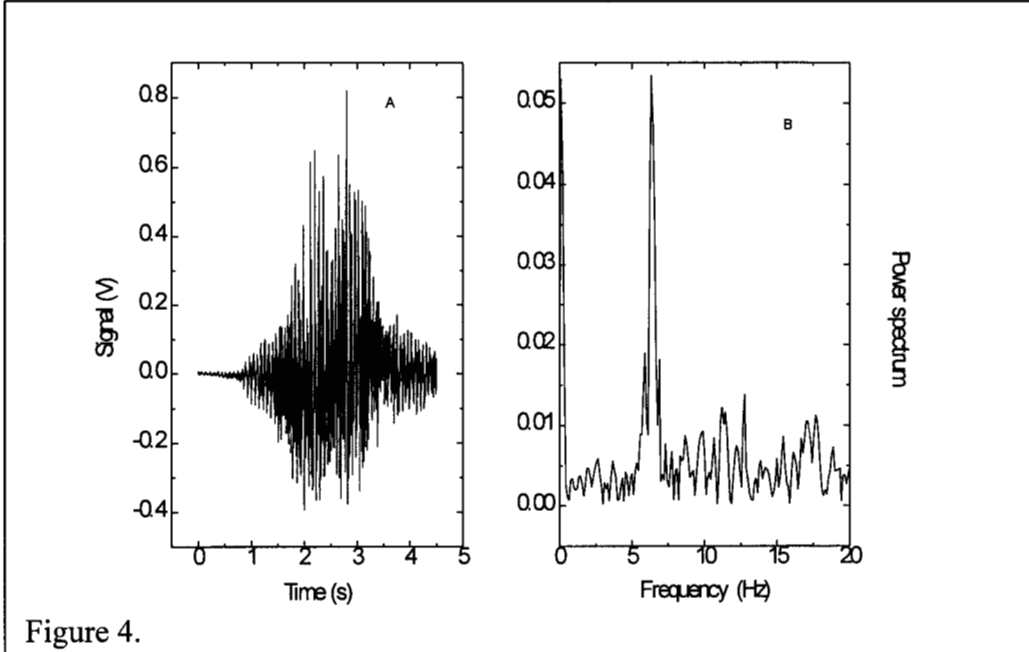


Figure 4.

driven by the Newport 850F actuator coupled to the Newport PMC-200 controller. The end of a 0.6  $\mu\text{m}$  diameter probe was dragged through the active area using aforementioned stages. The scattered light was focused through a lens onto a Si detector. The detector was connected to a current amplifier input; the output was connected to a PC using a National Instruments Lab-PC signal processing board.

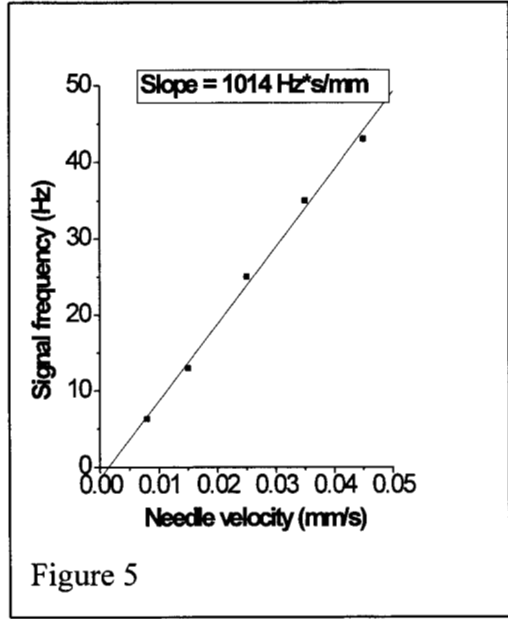


Figure 5

The spectrum of the measured signal was plotted and analyzed as shown in Figure 4. For speeds below 0.05 mm/s the Fourier transform of the signal yielded a distinct single peak as shown in Figure 4. At velocities above 0.05 mm/s very strong parasitic modes in the frequency region of interest appeared and obscured useful information. We found through additional experimentation that these are the vibrational modes of the needle and the needle holder that are excited when the stage is running. Therefore only data points for velocities below 0.05 mm/s were used to obtain velocity calibration. In Figure 5 we have plotted the frequency of the peak in the signal spectrum vs. the stage velocity. The linear fit of experimental data plotted as the peak

frequency vs. velocity yielded a slope of 1014 Hz/(mm/s). The expected slope of 1036 Hz/(mm/s) was calculated using Equation 2 with the laser wavelength of 0.66  $\mu\text{m}$  and angle  $\theta$  of 20°. This is in close agreement with the measured value.

## **Conclusions**

We have demonstrated a miniature illuminator for Laser Doppler velocimeter on micromachined optical bench utilizing a novel optical scheme. The device calibration yields the slope of the frequency/velocity dependence close to the theoretical prediction. The analysis of the active area suggests non-optimal focusing and alignment indicating that further work on the assembly and alignment techniques is needed.

## **Acknowledgments**

The research described in this paper was performed by the Center for Space Microelectronics Technology, Jet Propulsion Laboratory, California Institute of Technology, and was sponsored by the Directors research and Development Fund.

## **References**

1. F. Durst, R. Muller, and A. Naqwi. 'Semiconductor laser Doppler anemometer for applications in aerodynamic research'. *AIAA Journal*, 30 (4) pp. 1033-1038 (1992)
2. J. Seki 'Fiber-optic laser-Doppler anemometer microscope developed for the measurement of microvascular red cell velocity'. *Microvascular Research*, **40**, pp. 302-316 (1990)
3. H.W. Jentik, J.A. J. van Beurden, M.A. Heisdingen, F.F. de Mul, H. E. Suiches, J. G. Aarnoduse, and J. Greeve. 'A compact differential laser Doppler velocimeter using a semiconductor laser' 1987
4. T. Ito, R. Sawada, and E. Higurashi. 'Integrated microlaser Doppler velocimeter'. *J. Lightwave Technol.* **17** (1) pp. 30-34 (1999)
5. J.H. Lau. *Flip Chip Technologies*. (McGraw Hill, New York, 1996)
6. K. Petersen. "Silicon as micromechanical material". *Proc. IEEE* 70 (5) PP. 420-457 (1982)
7. P.W. Milonni and J.H. Eberly. *Lasers*. (John Wiley & Sons, New York, 1988)